Light Induced Electro-Luminescence Patterning: Interface Energetics Modification at Semiconducting Polymer and Metal-oxide Heterojunction in a Photodiode

Sanyasi Rao Bobbara,[†] Ehab Salim,[‡] Régis Barille,[¶] and Jean-Michel Nunzi[*,†,§]

[†]*Department of Physics, Queen's University, Kingston, ON - K7L 3N6, Canada.*

[‡]*Department of Physics, Faculty of Science, Mansoura University, 35516, Egypt*

[¶]*Department of Physics, Université d' Angers, Angers - 49045, France.*

[§]*Department of Chemistry, Queen's University, Kingston, ON - K7L 3N6, Canada.*

E-mail: nunzijm@queensu.ca

Phone: +1(613)533-6749

Experimental setup details

In this work, we attempted to bring multiple techniques together for an in-situ characterization of the device with spatial, temporal and spectral resolution, and to study the light-soak effects on the same device. Figure S1 shows the assembly of light sources, sensors and other electronics set up to study the current-voltage, charge-extraction by linearly increasing voltage (CELIV), photo and electro-luminescence, photovoltage and laser-beam induced current (LBIC) scan characteristics of the devices. The light-soaks were done with white light sources, mercury arc lamp and halogen lamp, switchable with a flip mirror mounted. The LBIC scan was performed using a diode laser at wavelength 532 nm that was triggered externally at 400 Hz and 50% duty cycle. The triggering signal source is used as a reference signal to the lock-in amplifier. With average optical power of $\sim 250nW$, photocurrent in the range of few nanoamperes was easily detectable using lock-in amplifier. A spatial resolution of about 2μm could be achieved with 10X objective of numerical aperture, although 0.5μm resolution is achieved with 100 X, 0.75 NA objective. The silicon photodiodes PD1 and PD2 are used to monitor the incident and reflected light intensity on and off the device, respectively. The rotatable filters turret (FS) in the microscope helps in easy switch between different filter-sets of choice for photo- and electro-luminescence tests. With flip mount (FM) in the baseport of the microscope, the optical signal from the device under test could be easily steered towards one or combination of ports with CCD camera for imaging or spectrometer or single photon counting and timing set-up.

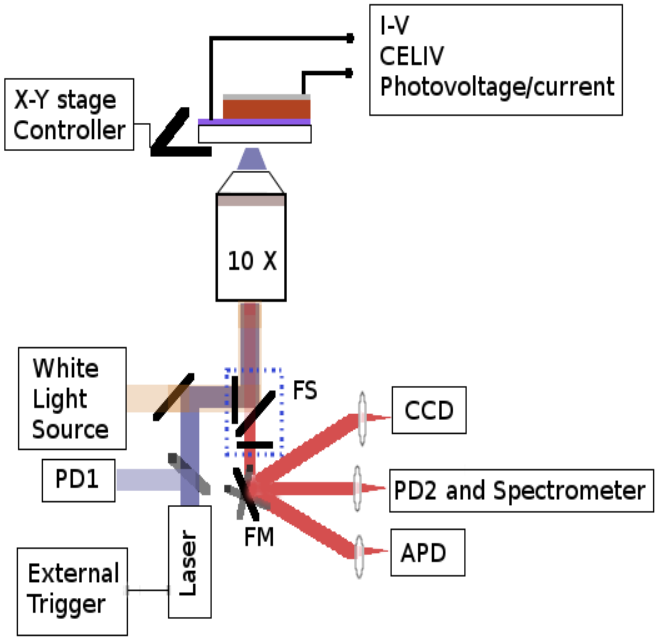

Figure S1: Experimental set-up employed to study the in-situ study of current-voltage, photo/electro-luminescence, CELIV, photovoltage, photocurrent LBIC scans of the devices. PD- photodiode, APD - avalanche photodiode, FS - filters set, FM - flip mount.

Effect of layers on device characteristics

Figure S2 shows the dark IV characteristics taken with and without various transporting/blocking layers such as ZnO and MoO_3 in the devices. With none of the buffer layers, the device is dominated by hole-only space-charge limited current (SCLC) for a relatively low voltage forward bias. The assymetric forward and reverse bias in the IV characteristics is from the difference in work function of indium tin oxide (ITO) and Silver electrodes. In the presence of ZnO, a rectification ratio as high as 10^4 at ± 1 V with very low leakage current was observed. MoO_3, a hole transporting layer, is contributing to additional series resistance (lower slope in IV in the SCLC regime) as well as to additional hole barrier at the anode obvious from the higher SCLC onset voltage.

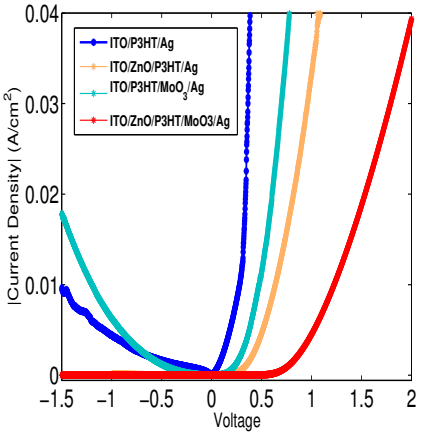

Figure S2: Current-Voltage characteristics of P3HT-based devices in the dark, with and without charge transport/blocking layers.

Figure S3 shows the effect of UV light-soak for 45 seconds on the device without MoO_3 i.e. of the form ITO/ZnO/P3HT/Ag. The UV exposure has led to an increase in electroluminescence efficiency, although it is not as efficient as the devices with MoO_3 layer. However, this test confirms that the enhancement in the EL observed is most likely associated with ZnO layer, and not with MoO_3.

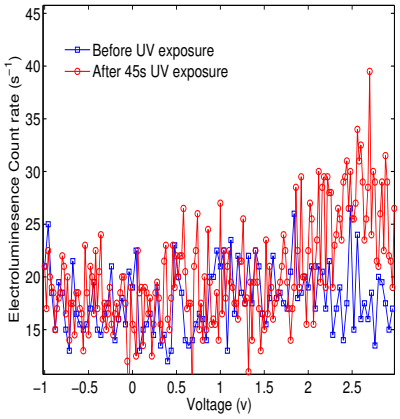

Figure S3: Electroluminescence versus bias voltage plot showing the effect of UV light-soak on a P3HT-based device without MoO_3 layer, ITO/ZnO/P3HT/Ag.

Characterization of Zinc Oxide Film

Figure S4 shows the absorption spectra of ZnO thin film on a glass substrate annealed at 180 ℃ for 30 minutes in air. The sharp cut-off at about 388 nm equivalent to energy bandgap of $\sim 3.19eV$ for ZnO thin film can be seen in it. Figure S5 shows the IPCE of the P3HT-based devices with and without ZnO layer and the absorption spectra of thin films of P3HT with ZnO and without ZnO layer on a glass substrate are also shown. ZnO aids in extracting higher photocurrent by collecting the electrons from the conduction band while blocking the holes from polymer valence band reaching the cathode, thereby reducing electron-hole recombination. This contribution can be seen with improved IPCE across the full range of absorption spectrum of P3HT. The photocurrent peak seen at about 360 nm is due to the electron-hole pairs generated in ZnO layer directly.

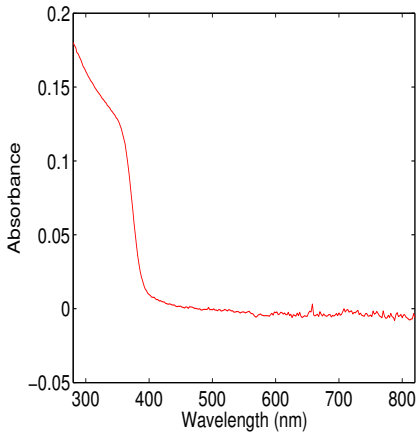

Figure S4: Absorption spectra of ZnO spin-coated on top of glass substrate and annealed at 180 ℃ for 30 minutes in air.

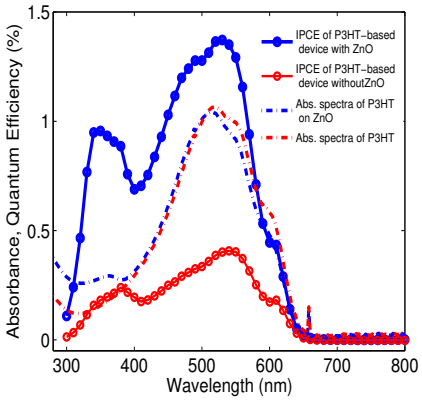

Figure S5: Incident photon to current conversion efficiency of the P3HT-based devices with and without ZnO layer and their corresponding absorption spectra.

Figure S6 shows the topography of a ZnO layer on top of ITO substrate annealed at 180 ℃ for the same 30 minutes measuring an average roughness, $R_a \sim 9nm$. The film thickness was measured to be about (40 ± 5) nm using Dektek profilometer.

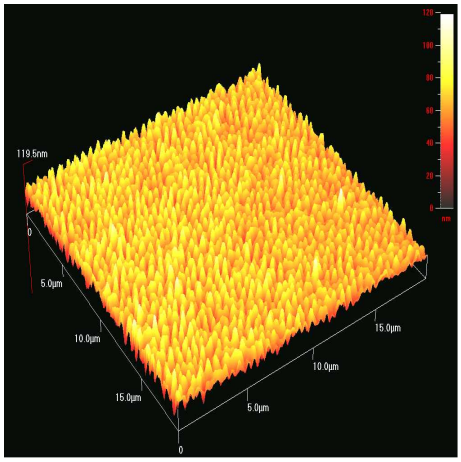

Figure S6: AFM scan of ZnO layer spin-coated on top of ITO(on glass) substrate and annealed at 180 ℃ for 30 minutes.

Figure S7 shows the FTIR spectra of ZnO films that were spin-coated on a bare glass substrate and annealed at two different temperatures, 150 ℃and 250 ℃for 30 minutes each. The spectra were recorded in attenuated total reflectance mode.

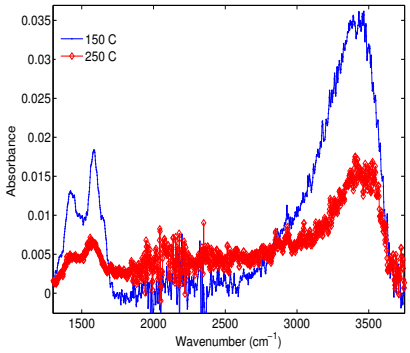

Figure S7: FTIR spectrum of ZnO film spin-coated on a glass substrate and annealed at 150 ℃and 250 ℃for 30 minutes.

PCDTBT-based device characteristics

The light-soak effects, similar to those observed in P3HT-based devices, were also witnessed in PCDTBT-based devices. The Figure S8 shows the dark-IV characteristics of PCDTBT-based device before and after light-soak.

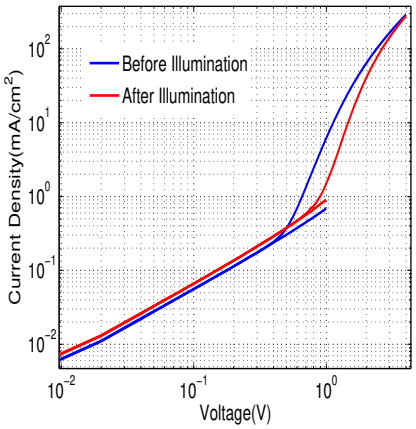

Figure S8: Current-Voltage characteristics taken in dark, before and after light-soak on a PCDTBT-based device.

Figure S9 shows the luminescence spectra off the PCDTBT-based device excited optically and electrically. The Electro-luminescence spectra is taken at 3 V after UV-light soaking for 3 minutes, and the photoluminescence spectra is taken with excitation wavelength $\lambda_{exct.} =$

405 ± 10 nm. The similarity of the spectra indicates that the electrically-injected charge recombination is occurring within the polymer.

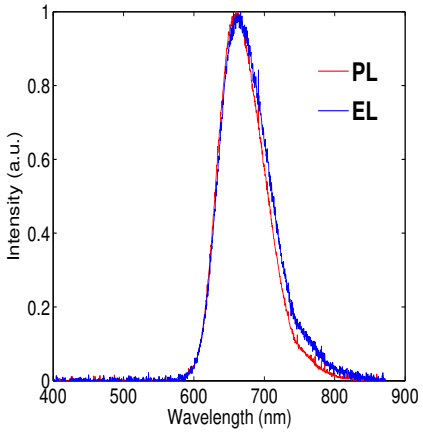

Figure S9: Photoluminescence (PL) and electroluminescence (EL taken after the light-soak and at 3 V forward bias) spectra of a PCDTBT-based device.